

Evidences Against Temperature Chaos in Mean Field and Realistic Spin Glasses

Alain Billoire

CEA/Saclay, Service de Physique Théorique, 91191 Gif-sur-Yvette, France.

Enzo Marinari

Dipartimento di Fisica and INFN, Università di Roma La Sapienza,
P. A. Moro 2, 00185 Roma, Italy.

(August 25, 2021)

We discuss temperature chaos in mean field and realistic 3D spin glasses. Our numerical simulations show no trace of a temperature chaotic behavior for the system sizes considered. We discuss the experimental and theoretical implications of these findings.

The problem of chaos in spin glasses has been under investigations for many years [1–9]. Even in the Sherrington-Kirkpatrick (SK) model, which is well understood with Parisi solution of the mean field theory [10], the possible presence or absence of temperature chaos is still an open problem. On the contrary, for example, chaos induced by a magnetic field h was already discussed by Parisi 15 years ago [1], and it is a clear feature of the Replica Symmetry Breaking (RSB) scenario. We will give here numerical evidences of the fact that, for all lattice sizes we are able to investigate by using state of the art optimized Monte Carlo method [11], there is no trace of temperature chaos in mean field (infinite range) and realistic spin glasses, in contradiction with previous claims [2,5–9]. The question about temperature chaos can be phrased by considering a typical equilibrium configuration at temperature T , and one (under the same realization of the quenched disorder) at $T' = T + dT$, where dT is small: how similar are such two configurations? In a chaos scenario for any non-zero dT the typical overlap would be exponentially small in the system size. We study both SK and Diluted Mean Field (DMF) [12] models. We consider the DMF model in its version with constant connectivity $c = 6$. Each lattice site is connected to c other sites chosen at random. It is interesting to check if this model has the same features as the SK model. We also study the 3D Edwards Anderson (EA) realistic spin glass. In all models spin variables are Ising like ($\sigma = \pm 1$), and the couplings J can take the two values ± 1 with probability $\frac{1}{2}$. Our Monte Carlo dynamics is based on *Parallel Tempering* (PT) [11]: we run in parallel two sets of copies of the system, and always take overlap of configurations from two different Markov chains. We use all standard precautions for checking thermalization of our data [11]. The indicator of a potential chaotic behavior will be the two temperature overlap $q_{T',T}^{(2),(N)} \equiv \langle \left(\frac{1}{N} \sum_{i=1}^N \sigma_i^{(T)} \tau_i^{(T')} \right)^2 \rangle$. The usual square overlap $q_{T,T}^{(2),(N)}$ is a special case of $q_{T',T}^{(2),(N)}$.

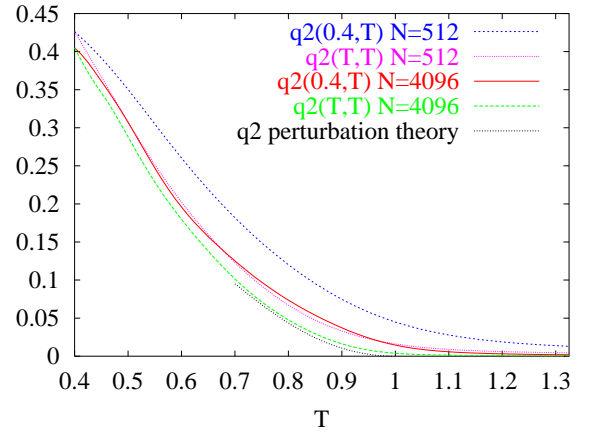


FIG. 1. $q^{(2)}$ at equal and different T values for the SK model, with $N = 512$ and $N = 4096$ sites. The lower curve is the perturbative result for equal T $q^{(2)}$. See the text for details.

Let us start from the analysis of our data for the SK model. In figure 1 we plot the square overlap for the two temperature values $(0.4, T)$ (i.e. the overlap of a copy of the system at temperature $T' = 0.4$ with a copy of the system at $T \in (0.4, 1.35)$), and the one at equal temperature (T, T) . The two upper (on the left side of the plot) dashed curves (merging at $T = 0.4$ at a value close to 0.42) are for $N = 512$ spins (a small lattice size), the upper one being the $(0.4, T)$ curve and the lower one the (T, T) one. The two lower curves (merging at $T = 0.4$ at a value close to 0.40) are for $N = 4096$ (our largest lattice for the SK model): of these two lower curves the solid, upper curve is for $(0.4, T)$, while the dashed lower one is the (T, T) $q^{(2)}$. The fifth curve from the top, that stops down at $T = 0.7$ is the perturbative result for $q_{T,T}^{(2),(\infty)}$ [13] (useful for checking our numerics and the quality of the approach to the asymptotic large volume limit). Here we only plot data from two lattice sizes, and do not show the statistical errors that are small enough not to affect any of the issue discussed here, but would make the picture

less readable. We show data for the lowest temperature we have been able to thermalize, $T' = 0.4$. The same qualitative picture holds for larger T' values ($T' < T_c$).

One notices at first glance from figure 1 that for both N values (and, as we will see, for all N values and different systems we have analyzed) $q_{0.4,T}^{(2),(N)} \gtrsim q_{T,T}^{(2),(N)}$ ($T \geq 0.4$). This is what happens in a non-chaotic systems (for example ferromagnets where $q_{T',T}^{(2),(N)} = M(T)^2 M(T')^2$, where $M(T)$ is the magnetization at temperature T), and is very different from what would happen in a system with T -chaotic states. The second crucial observation is that the distance between $q_{0.4,T}^{(2),(N)}$ and $q_{T,T}^{(2),(N)}$, at fixed $T > 0.4$, decreases with N , the two curves even seem to collapse at large N . This kind of behavior shows the absence of temperature chaos in the Sherrington-Kirkpatrick system and, as we will discuss in the following, in the diluted mean field and 3D EA spin glasses. This evidence, together with an understanding of the physical mechanism that is at the origin of this behavior (thanks to the analysis of $P(q)$) is the main point of this note.

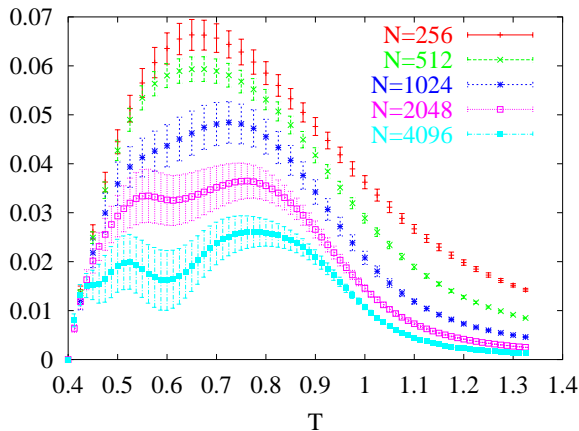


FIG. 2. $q_{0.4,T}^{(2),(N)} - q_{T,T}^{(2),(N)}$ as a function of T for the SK model with different N values.

A more quantitative evidence comes from figure 2, where we plot $q_{0.4,T}^{(2),(N)} - q_{T,T}^{(2),(N)}$ as a function of T for the SK model with $N = 256, 512, 1024, 2048$ and 4096 . Here the errors are computed by an analysis of sample to sample fluctuations (it is important not to forget that the points for different temperatures are strongly correlated, since they involve the same $T = 0.4$ data, or data from different temperatures but nevertheless from the same PT simulation). In the large volume limit both contributions to the difference are zero for $T > T_c = 1$, so that the non zero value of the curves in this regime gives us a measure of finite size effects. Large lattices have larger fluctuations. This is connected to the non-self-averageness of $P_J(q)$: the peaks of $P_J(q)$ become narrower for large lattices (eventually approaching δ -functions in the large volume limit), and averaging them to compute expecta-

tion values of the overlap gives a wiggling behavior, that becomes smooth only for a very large number of disorder samples. We are not able to keep under control a precise fit of the data of figure 2 for $N \rightarrow \infty$, but the strong decrease of the difference of the data at large N is clear, and the possibility that the limit is zero everywhere looks very plausible (it would be very interesting to understand theoretically this behavior).

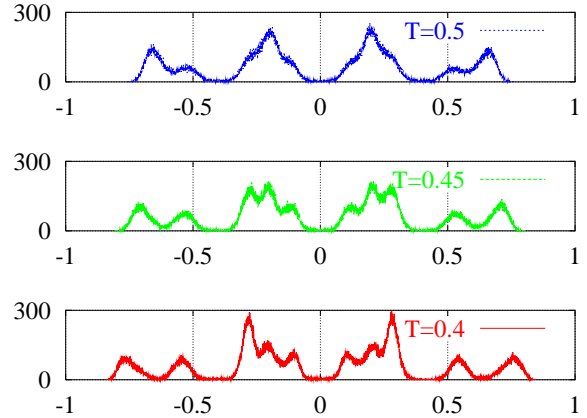


FIG. 3. $P_J(q)$ for the same selected disorder realization at three different temperatures of the SK model with $N = 4096$ sites.

We use figure 3 for trying to understand better the mechanism governing how stable states of the system vary as a function of T . We plot the probability distribution $P_J(q)$ for a given disorder realization of the SK model with $N = 4096$. We show, from top to bottom, the results at $T = 0.50, 0.45$ and 0.40 . The function $P_J(q)$ should be symmetric around $q = 0$, since we are at zero magnetic field. The level of symmetry reached by our finite statistics sample is a measure of the quality of our thermalization: from figure 3 it looks very good. Note that there is no peak close to, or at, the origin: this disorder realization carries little weight in the $q \simeq 0$ region. At the lowest T value there are 5 peaks for positive q , three of which very well separated. It is interesting to follow the evolution of $P_J(q)$ from $T = 0.50$ down to $T = 0.40$. At $T = 0.50$ there are basically two very broad peaks, that get resolved at $T = 0.45$: one broad peak gets divided in two clear peaks (that become very clear at $T = 0.4$), while the other forms a 3 peak structure, that get different weights at $T = 0.4$. What one sees in figure 3 is interesting since it constitutes a typical pattern: when lowering T , states start to contribute to the $P_J(q)$ by bifurcations (new peaks emerge) and by smooth rearrangements of the weights. One never sees dramatic changes involving strong redistributions of weight among far away peaks, that would be typical of a chaotic situation: the phase space is obviously very complex, as it has to be in a situation characterized by RSB [10], but

the T -dependence of the phase space is smooth and non chaotic.

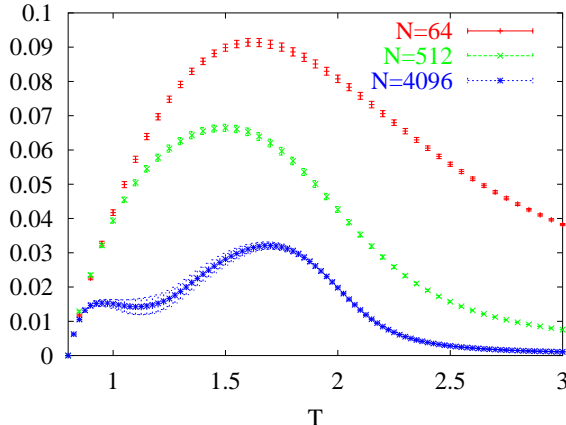


FIG. 4. As in figure 2, but DMF, $N = 64, 512$ and 4096 .

The situation in the DMF model (where $T_c \simeq 2.07$) is very similar to the one in the SK model. In figure 4 we show the analogous of figure 2, for $N = 64, 512$ and 4096 spins. The two figures are very similar, and even the size of the difference we are plotting is very similar in the two models, when comparing the same values of N . The situation in the DMF model looks exactly the same of the SK model: there is no temperature chaos.

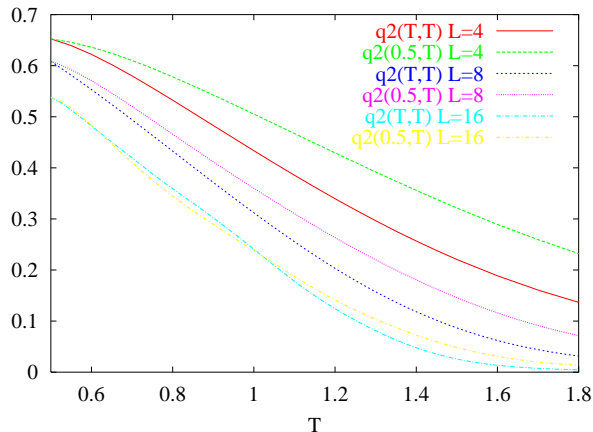


FIG. 5. $q^{(2)}$ at equal and different T values for the 3D EA model.

The situation in the 3D EA model is different only in that finite size effects are very large (this is well known from numerical simulations [14]). In figure 5 we show $q^{(2)}$ at equal and different T values for $L = 4, 8$ and 16 . It is clear that $q^{(2),(N)}$ decreases noticeably with $N = L^3$ for all values of T . It is also remarkable that even at very large T values (with T far larger than the estimated value of $T_c \simeq 1.16$ [15,16]) $q^{(2),(N)}$ is different from zero even at $N = 4096 = 16^3$. Apart of that figure 5 shows a

situation very similar to the one of 1. We are definitively not in a situation where $q_{0.4,T}^{(2),(N)}$ goes to zero exponentially and $q_{T,T}^{(2),(N)}$ goes to a non zero limit (even if the distance between the two curves for $L = 16$ has become very small, and even negative in a temperature region). In figure 6 we show the 3D analogous of figures 2 and 4. Again, even for $T > T_c$, on the smaller lattices one has non-zero differences: finite size effects are large, but apart from that the emerging picture is analogous to the one we have found in mean field (diluted and not).

Now, before discussing the data, we give a few details about our runs. For the SK model we use $T_{min} = 0.4 = 0.4T_c$. We simulate $N = 256, 512, 1024, 2048$ and 4096 : for the different N cases we have from 26 to 142 samples, a set of from 38 to 75 temperature values with a dT going from 0.025 to 0.0125. We run 200000 sweeps but for the $N = 4096$ and $N = 2048$ lattices where we run 400000 sweeps (we always use for measurement only the second part of the run). For the DMF model we have $T_{min} = 0.8 \simeq 0.4T_c$. We use from 640 to 1024 samples for $N = 64, 512$ and 4096 . Here T_{max} is 3, the number of temperatures from 45 to 89 and the number of iterations from 100000 to 200000. In the 3D EA model we use $T_{min} = 0.4, T_{max} = 2.075$ (here $T_c \simeq 1.16$) and a dT going from 0.050 to 0.025. We have 1344 samples for $L = 4$ (200000 sweeps) and $L = 8$ (300000 sweeps), and 64 samples for 16^3 (where $T_{min} = 0.5$, with 3450000 sweeps, this is very many sweeps of many tempering copies). Our SK program was multi-spin coded on different sites of the same system (we store 64 spins of the system in the same word), while the DMF and 3D codes are multi-spin coded on different copies of the system [17]. We want to note that, as compared to previous numerical simulations, we have been able (thanks to a large computational effort and to the use of PT) to thermalize the systems at very low T values. It is also interesting to notice that in the $N = 4096$ case the 3D EA model requires many more sweeps than the DMF and the SK model.

In all our simulations we do not observe any temperature chaos effect. This is true for the SK model, the diluted mean field and the 3D EA model: the three models behave very similarly. The differences we have plotted, that would decrease exponentially in a chaotic scenario, do not decrease faster than logarithmically. Obviously from our numerical findings we cannot be sure that things will not change for very large system sizes, but again, we can claim that the absence of any temperature chaotic behavior is crystal clear on our lattice size. Two final comments are in order. At first, as we already said, we cannot be sure about the behavior in the very large system limit: the difference of $q_{T',T}^{(2)}$ and $q_{T,T}^{(2)}$ (for $T' \simeq 0.4T_c$ and $T > T'$) decreases with the system volume, and is close to zero on the larger lattice sizes we can simulate. This difference could eventually become negative, and the correlation at $T \neq T'$ could eventually drop exponentially

on very large lattices: we can only say we do not see any trace of that. The second comment is that, in any case, our results have an experimental relevance: the number of spins that are equilibrated during a real experiment is of an order of magnitude only slightly larger than the order of magnitude of the one we can thermalize in our numerical simulations [18], so our results strongly suggest the absence of temperature chaos in real experiments.

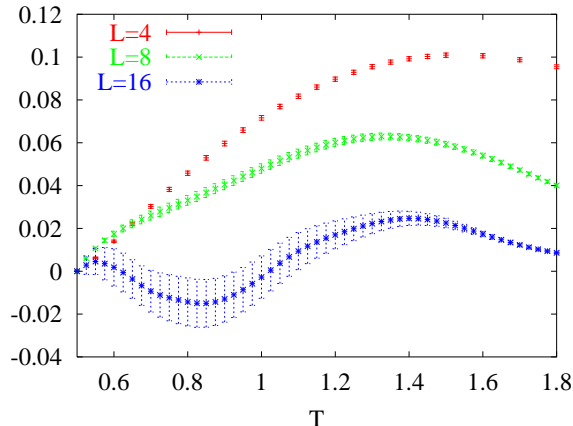


FIG. 6. $q_{0.5,T}^{(2),(N)} - q_{T,T}^{(2),(N)}$ as a function of T for the 3D EA model with different L values.

The previous work of other authors on chaos was pointing toward the presence of temperature chaos. On one side in this context the analytic computations have by no means an unambiguous meaning, since they are based on strong assumptions or on a perturbative and/or approximate treatment. On the other side numerical computations of older generations were much limited in scope as compared to what we can do now. For example Ritort numerical computation [7], that was correctly, in the limit of the gathered data, finding chaos, was looking at a T starting value of 0.4, and a dT of 0.5 (as compared to the 0.0125 we have been able to use here), i.e. was comparing $T = 0.4$ to $T = 0.9$ (where $T_c = 1$) on reasonably small lattice. In this case the decrease of the overlap is clear, but turns out to be due to finite size effect (since even the equal T overlap has to go to zero at T_c).

A last comment (following for example [19]) is about the relevance of the absence of chaos for the description of realistic, finite dimensional spin glasses. In short the absence of a temperature chaotic behavior makes impossible a modified droplet like description of realistic spin glasses (the original droplet model cannot work for example because of the observed dynamical scaling of the energy barriers).

Following [19] one notices that the very weak dependence of spin glass physical properties on the cooling rate is not plausible in a scenario of activated domain growth. Only arguing that there is temperature chaos one can reconcile the negligible effect of the cooling rate with a

droplet picture. The absence of temperature chaos makes this reconciliation impossible.

We are aware that G. Parisi and T. Rizzo in a perturbative computation close to T_c find absence of temperature chaos (at the order they do compute, but not necessarily at all orders in perturbation theory), both in the SK and in the DMF model. S. Franz and I. Kondor have connected evidence that excludes temperature chaos at lowest orders close to T_c . We deeply thank all of them, together with J.-P. Bouchaud and F. Ritort, for interesting conversations. The numerical simulations have used, together with a number of workstations, computer time from the Grenoble T3E Cray and the Cagliari Linux cluster Kalix2 (funded from Italian MURST under a COFIN grant).

-
- [1] G. Parisi, *Physica A* **124**, 523 (1984).
 - [2] A.J. Bray and M.A. Moore, *Phys. Rev. Lett.*, **58**, 57 (1987).
 - [3] K. Binder and A.P. Young, *Review of Modern Physics* **58**, 801 (1986).
 - [4] I. Kondor, *J. Phys. A: Math. Gen.* **22**, L163 (1989).
 - [5] M. Ney-Nifle and H. J. Hilhorst, *Physica A* **193**, 48 (1993).
 - [6] I. Kondor and A. Végso, *J. Phys. A: Math. Gen.* **26**, L641 (1993).
 - [7] F. Ritort, *Phys. Rev. B* **50**, 6844 (1994).
 - [8] S. Franz and M. Ney-Nifle, *J. Phys. A: Math. Gen.* **28**, 2499 (1995).
 - [9] M. Ney-Nifle, *Phys. Rev. B* **57**, 492 (1998), cond-mat/9707172.
 - [10] M. Mézard, G. Parisi and M. A. Virasoro, *Spin Glass Theory and Beyond* (World Scientific, Singapore 1987).
 - [11] See for example E. Marinari, in *Advances in Computer Simulation*, edited by J. Kerstész and I. Kondor (Springer, Berlin 1998), p. 50, cond-mat/9612010.
 - [12] J. R. Banavar, D. Sherrington and N. Surlas, *J. Phys. A* **20**, L1 (1987); M. Mézard and G. Parisi, *Europhys. Lett.* **3**, 1067 (1987).
 - [13] H. J. Sommers, *J. Physique* **46**, L779 (1985).
 - [14] E. Marinari, G. Parisi and J. Ruiz-Lorenzo, in *Spin Glasses and Random Fields*, edited by P. Young (World Scientific, Singapore 1998), p. 59, cond-mat/9701016.
 - [15] N. Kawashima and A. P. Young, *Phys. Rev. B* **53**, R484 (1996), cond-mat/9510009.
 - [16] M. Palassini and S. Caracciolo, *Phys. Rev. Lett.* **82**, 5128 (1999), cond-mat/9904246.
 - [17] H. Rieger, *J. Stat. Phys.* **70**, 1063 (1993), hep-lat/9208019; our code is based on F. Zuliani (1998), unpublished.
 - [18] Y. G. Joh et al., *Phys. Rev. Lett.* **82**, 438 (1999), cond-mat/9809246.
 - [19] J.-P. Bouchaud, L. F. Cugliandolo, J. Kurchan and M. Mézard, in volume cited in [14], p. 161.